Journal of Engineering Science and Technology
Vol. 15, No. 1 (2020) 291 - 304

WATER SURFACE PROFILE AND FLOW PATTERN SIMULATION OVER BRIDGE DECK SLAB

SHAYMAA A. M. AL-HASHIMI, SANAA A. T. AL-OSMY, SAAD MULAHASAN*

Department of Water Resources Engineering, Mustansiriyah University, Baghdad, Iraq
*Corresponding Author: Shmulahasan@uomustansiriyah.edu.iq

Abstract

During large flooding events, a bridge deck subjected to hydrodynamic loading. In such extreme events, bridges exposed to a full orifice flow and overtopping and may cause extensive damage. A bridge deck is physically modelled using Cardiff University's 10 m long, 30 cm wide and 30 cm deep laboratory flume. The bridge model consists of an abutment with a continuous bridge slab with a blockage ratio of 0.3. A Computational Fluid Dynamics (CFD) technique is used to numerically simulating fluid flow behaviour in the vicinity of a bridge deck. The simulation focuses on the water surface profiles and longitudinal velocity field through a partially-full orifice flow and an entirely inundated bridge deck of rectangular shape and the interference of the main flow with the structure of the bridge opening in an open channel. The numerical model employed the equations of continuity and momentum with the Re-Normalization Group RNG (k-ε) turbulent model. The volume of fluid method is used to predict the water surface profiles. Good agreement was observed between the numerical simulation and the predicted water surface profiles. The obtained water surface profiles for the different examined flow discharges show similar trends; they rise upstream to form the backwater profiles and show a sudden drop through the bridge contraction. The CFD model results indicate a slightly overestimate in the water depths of the hydraulic jump on the bridge downstream side due to the critical flow condition. In addition, longitudinal velocity fields are extracted around the structure.

Keywords: ANSYS fluent, Bridge, Computational fluid dynamics (CFD), Open channel, Water surface profile.

1. Introduction

During large flooding events, a bridge deck is subjected to hydrodynamic loading. In such extreme events, bridges exposed to a full orifice flow and overtopping and may cause extensive damage. The bridge in an open channel triggers a very high turbulent flow field containing 3D complex coherent structures around bridge structures [1]. Under these conditions, bridges become partially or entirely submerged and the hydrodynamic forces acting on the bridge become critical, leading to stability problems for the existing structure [2, 3]. Guo et al. [3] examined the hydrodynamic-loading and six an inundated girder bridge deck model. The experimental data was also used to analyse the validation of complementary numerical simulations. Velocity distributions were analysed using a PIV technique. Different scale- factors were used to analyse the scaling effect on hydrodynamic loading. The exerted forces by the flow under a fully inundated bridge deck is studied by a number of researchers and specified by a drag equation with a constant drag coefficient. The drag coefficient is dependent on the projected area of the deck or the pier [4, 5]. The hydrodynamic loading on rectangular section channel with bridge deck with different submergence levels and different deck Froude numbers was examined [4].

Numerous studies have investigated bridges piers and abutments under flood loading subjected to scour [6-8]. In addition, the bridge and abutments, which act as obstacles, cause backwater at the upstream part of the bridge. Backwater surface profiles lead to changes in the flow field, especially around the bridge and abutment [9-11]. Equations for backwater and discharge for flows through partially or fully-submerged rectangular bridge decks were derived [10]. The water-surface profiles formed as a result of the presence of different bridge-structures were investigated [11], their study investigated three cases: a cylindrical pier, a deck, and a cylindrical pier with deck. Their study focused on the deck and - bridge cases. In addition, flow velocity was measured by a PIV system. 3D Reynolds-Averaged-Navier-Stokes (RANS) model and the simulation of these cases was done by (k-ε) turbulence closure. Good agreement was obtained between experimental work and simulations.

Over the past two decades, frequent employment of computational models has resulted in large developments in computer science. CFD models are becoming commonplace and are important when employed to hydraulic engineering problems. Numerical models have been used to predict the free surface profiles and flow patterns in open channel flows in the vicinity of obstacles [12-15]. A numerical 3D flow and localized scour around a non-submerged spur dike was studied [12], where Navier-Stokes equations were solved using a finite volume method.

Large Eddy Simulation (LES) method was employed to accurately predict the 3D turbulent flow around bridge structures, [13, 14]. The LES code was refined with a novel free surface algorithm based on the Level Set Method (LSM) for determining the complex water surface profiles. The code was used to analyse the hydrodynamics of compound channel flow with deep and shallow over banks, free flow around a bridge abutment, pressure flow with a partially submerged bridge deck and bridge overtopping flow. All simulations were validated with data from complementary physical model tests at Cardiff University under analogous geometrical and flow conditions. Primary velocity, bed shear stress, turbulence

characteristics and 3D coherent flow structures were examined thoroughly for each of the flow cases to explain the hydrodynamics of these complex turbulent flows.

The flow patterns around a single spur dike and the free surface flows using a fluent numerical model were simulated. Based on other studies obtained by Yazdi et al. [15], good agreement was observed between the free surface and velocities of the 3D model and three experimental data sets. Method of Lattice Boltzmann for flutter analysis of the bridge decks were used [16]. They developed a fluid structure interaction algorithm within the framework of the multiple relaxation times Lattice Boltzmann Method. To demonstrate the application of the presented algorithm, flutter analysis of the Second Forth Road Bridge and the River Bridge of Guamá were studied. A comparison between the numerical results with wind tunnel measurements shows that there is a good prediction of the flutter onset velocities of the Forth Road Bridge and the Guamá River Bridge. Thus, indicating, the applicability of the presented and used algorithm. The validation of a 3D Morpho-dynamic model for complex flows using Large Eddy Simulation was studied [17]. His study aimed to present the testing and validation of an up-to-date three-dimensional CFD model, REEF3D, developed at the Norwegian University of Science and Technology, through the numerical modelling of complex free surface flows and sediment transport. Kara et al. [13, 14] develop his numerical model, which was set up based on a physical model.

The study examined a more complex flow problem, namely high discharge flow through a submerged bridge with overtopping. The validation of a 3D CFD model, which was used to calculate the water surface profile over a trapezoidal broad crested weir was examined [18]. The results were compared with experimental data from a physical model for different discharges. Good agreement was shown between the numerical and the physical models. Different flow types (free-surface, submerged orifice, and overtopping) were experimentally investigated to abutment local scouring [19, 20]. Results showed that abutment scour can be influenced by lateral and vertical flow contraction effects in the cases of overtopping, submerged and free surface flows. Research papers seem to be so rare in the field of extreme flooding events to bridges.

The aim of present study is to investigate three-flow types (free surface, full-orifice and overtopping) effect on water surface profiles and velocity fields in turbulent open channel flow in the vicinity of a bridge with side abutments and deck slab. Different open channel flow conditions are simulated using a commercial CFD tools. The water surface profile was determined by using the Volume of Fluid (VOF) method. The most important case found that under high flow rates, bridges might become submerged partially or completely submerged. Therefore, it is very important to determine the free surface elevation in order to understand the effect of the water surface profile on the flow characteristics.

2. Experimental Setup

The physical model experimental works were carried out in Cardiff University ’s, Laboratory of hydraulics using tilting flume with dimensions of (10 m in length, and 0.30 m in width) while a bed slope was set to (1/2000). These experiments were used to calculate the water surface profiles featuring a bridge model [21]. The bridge model was considered under two flow cases; overtopping and full orifice flow. For the case of overtopping flow, the model bridge consisted of an abutment with (10 cm length, 9 cm width, and 5 cm height) and a rectangular bridge deck 2.4

cm thick, which extends across the channel. For the case of orifice flow, an opening area (21 cm by 5 cm and 10 cm length) was considered.

To make comparison with the numerical results, the overtopping flow rates were (Q = 7.0 L/s, 8.5 L/s, 12. 0 L/s and 15.0 L/s), with corresponding uniform flow depths (H = 7.98 cm, H = 9.20 cm, H = 9.93 cm and H = 11.53 cm) were applied respectively. One of these overtopping flow coditions which is (Q = 8.5 L/s) had been done by Kara et al. as explained in reference [14]. For the case of flow occurring along the entire bridge, with the upstream level of water below the bridge deck upper edge, the flow was said to be of the (full-flow-orifice) full orifice flow type. A single flow rate, with a discharge of (4.50 L/s), was considered for such a flow type. Measurements of water level depths were taken along the central (mid) width of the flume for both cases.

Table 1 describes the flow conditions for the orifice full flow and the overtopping cases, where w is the flume width, (V_{uni}) is the velocity under uniform flow conditions, (H) is the uniform depth of flow, h is the water level depth along the flume, (g) is the acceleration due to gravity, (υ) is kinematic viscosity, Re is Reynolds number and Fr is Froude number. Table 1 provides a summary of flow conditions for two flow types (submerged and overtopping). It seems that Reynolds number was in the range of (23200 ≤Re≤ 49800) and Froude number was in the range of (0.34-0.41) for the overtopping flow cases and (Re =14940 and Fr = 0.37) for the submerged flow case. Such types of flows state turbulent subcritical flows.

Table 1. Flow conditions for orifice full flow and overtopping cases.

Flow case	Q	H	w	V_{uni}	Re = $V_{uni}H_{uni}$/ν	Fr = V_{uni}/$(gH)^{0.5}$
	(m^3/s)	(cm)	(cm)	(m/s)	(-)	(-)
Overtopping	0.0150	11.53	30	0.434	49801	0.383
Flow	0.0120	9.93	30	0.403	39841	0.414
	0.0085	9.2	30	0.308	28220	0.341
	0.0070	7.98	30	0.292	23240	0.374
Orifice flow	0.0045	6.4	30	0.234	14940	0.373

3. CFD Modelling

In this study, the simulation focused on the application of the commercial (CFD) software - (ANSYS fluent), to predict the longitudinal velocity field and water surface profiles on flooded- bridge deck for different values of discharges through application the following functional models [22]. The governing contiuity and momemtum equatios of flow are as follow:

$$\frac{\partial \rho}{\partial t} + \nabla(\rho u) = 0 \quad (1)$$

$$\frac{\partial}{\partial t}(\rho u) + \nabla(\rho u u) = -\nabla p + \nabla \tau \quad (2)$$

where ρ and u are fluid density and velocity respectively, p is pressure, t is time and τ is shear stress.

In order to simulate turbulent flow around a bridge deck, turbulence model is a common two-equation should be employed, that is used as a closure for the Reynolds-Averaged-Navier-Stokes (RANS) equations. The improving of (k-ε) turbulence model, which called the (RNG) (Re-Normalization Group) (k-ε) model

was presented [23], where the coefficients cannot be obtained from the experimental work, instead, from theoretical analysis. The RNG (k-ε) model has better applicability than (the standard (k-ε) model). Their study uses the (RNG k-ε) model to simulate the flow turbulence of the bridge deck, in conjunction with the (standard wall- function method) to deal with the near wall. The equations, which govern the flow, are as follows [23]:

$$\frac{\partial k}{\partial t} + u_j \frac{\partial k}{\partial x_i} = \tau_{ij} \frac{\partial u_i}{\partial x_j} + \frac{\partial}{\partial x_j}\left[\frac{1}{\rho}\left(\mu + \frac{\mu_t}{\sigma_k}\right)\frac{\sigma_k}{\partial x_j}\right] - \in \tag{3}$$

$$\frac{\partial \varepsilon}{\partial t} + u_j \frac{\partial \varepsilon}{\partial x_i} = \mathrm{C}_{1\varepsilon} \frac{\varepsilon}{k} \tau_{ij} \frac{\sigma u_i}{\sigma x_j} + \frac{\sigma}{\sigma x_j}\left[\frac{1}{\rho}\left(\mu + \frac{\mu t}{\sigma k}\right)\frac{\sigma \varepsilon}{\sigma x_j}\right] - \mathrm{C}_{2\varepsilon}\rho \frac{\varepsilon^2}{k} \tag{4}$$

where k is turbulent kinetic energy, ε is the turbulent kinetic energy dissipation, μt is turbulent eddy viscosity, τ_{ij} is Reynolds stress. The constants are: $C\mu$ = 0.085, $C_{1\varepsilon}$ = 1.42, $C_{2\varepsilon}$ = 1.68, σk = 0.7179 and $\sigma \varepsilon$ = 0.7179 [22].

Grid system and numerical methods

The three-dimensional (CFD) model scale factor was 1:1 - the same dimensions of the experimental setup. The deck was located at a distance 6.4 m downstream from the channel inlet where a uniform velocity was set at the channel inlet, (see Fig. 1). The flow depth varies with discharge.

The bridge deck height measured from the bottom of the channel was (50 mm). The bridge-deck dimensions used in the simulation model analysis were of the same dimensions of the experimental work. The three-dimensional models of the bridge deck were designed using the GAMBIT program; a geometrical construction and grid generation tool. Since the flow near the bridge is more complex, the grid was refined to suit. A generation of multi-block grid technique was used.

The grid cells near the bridge deck were (3 mm) and increased to (2 cm) away from the bridge deck. A (3D) grid system with (227,428 nodes) and (1,122,818 cells) was generated using GAMBIT. The bridge 3D-geometry with boundary conditions that applied in program is presented in Fig. 1(b). Pressure inlet is used for inlet while pressure outlet employed for outlet. Walls are applied for all sides of flume and bridge and free surface is applied for the water surface in channel.

Generally, the steps involved creating the numerical model in GAMBIT for the geometry of the flume and the bridge deck and defining the boundary conditions. The grid contains two zones, water zone and air zone. A volume of fluid (VOF) multiphase model was used to find the flow in the open channel as well as the constituent elements of the free surface for the specified inlet and outlet conditions. The VOF method was also used to determine the water surface profile by calculating the water level in each control volume [24]. The volume of water fraction in each control volume must equal unity; if it contains only water (α_w) = 1, it contains only air (α_w) = 0, and if it is in between $0 \leq (\alpha_w) \leq 1$, where (α_w) is volume of water fraction. The geometry grid in the VOF method domains was from 0 to 1 (see Fig. 2).

For other conditions where the flow was no longer transient, the RNG (k-ε) turbulence model was used. The pressure discretization was applied since the flow was gravity driven. Second order discretization was used for momentum, dissipation and turbulence kinetic energy equations and PISO pressure-velocity coupling was employed.

(a) A photograph illustrating the experimental set-up.

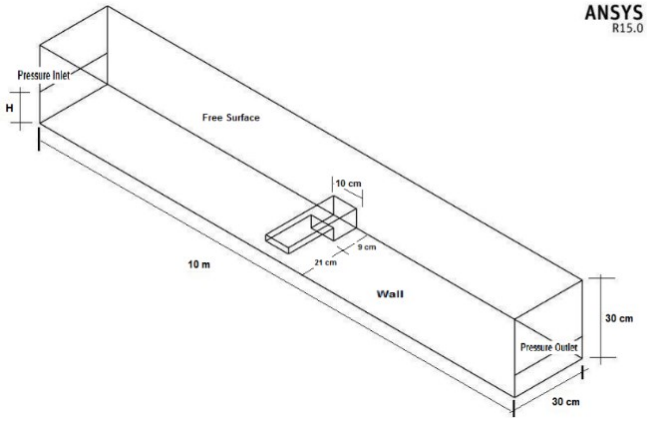

(b) Three-dimensional CFD geometry illustration of bridge deck-slab.

Fig. 1. Bridge model layout.

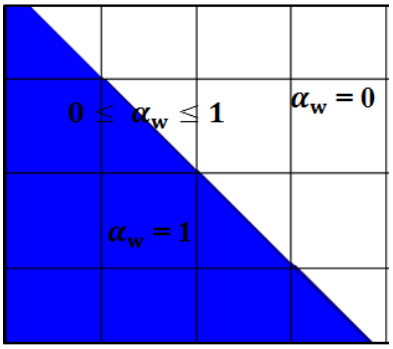

Fig. 2. Mesh with a volume of water fraction [23].

4. Results and Discussions

Based on studies by Yoon et al. [20], CFD numerical model was used to examine conditions under the five discharge scenarios (4.5 L/s, 7 L/s, 8.5 L/s, 12 L/s and 15

L/s) that were used in the laboratory flume experiments and featured the bridge model. Results are highlighted as water surface profiles and velocity field for two flow categories of full orifice flow and overtopping flow. Water surface profile results are shown in a non-dimensionalised form in Figs. 3 and 4(a) to (d). Figure 3 shows the relation between water level height (h) along the flume length in each distance (x) for the oriface flow case with flow through the bridge of (Q = 4.5 L/s). Water level has been normalized on the flow uniform depth H, while the distance along channel length (x) was normalized on the channel width (w). Good agreement was observed between the numerical and the experimental data. In addition, a little distance from the bridge deck the water is backed up by a significant amount and the CFD predicts this very well.

For the overtopping case studies, the streamwise water surface profiles were compared with the experimental data. As expected, the free surface profiles were one of the most complex features of this study. The water surface profiles obtained from four different flow discharges (7 L/s, 8.5 L/s, 12 L/s and 15 L/s) show similar trends; they rise upstream to form the backwater profiles and then show a sudden drop through the bridge contraction. For the overtopping case studies, the streamwise water surface profiles were compared with the experimental data. As expected, the free surface profiles were one of the most complex features of this study. The water surface profiles obtained from four different flow discharges (7 L/s, 8.5 L/s, 12 L/s and 15 L/s) show similar trends; they rise upstream to form the backwater profiles and then show a sudden drop through the bridge contraction.

Further downstream these profiles fluctuate, and normal depth was reached at the downstream end of the channel. Generally, the profiles obtained from the CFD model show good agreement with that of the experimental data (Figs. 4(a) to (d). A little distance from the bridge the water is backed-up by a significant amount and the CFD predicts this very well as with the orifice flow study case. There was a significant shift between the numerical and the experimental cases at the downstream location at (12 L/s and 15 L/s) discharges (Figs. 4(c) and (d)). This is because, under turbulent conditions, it is difficult to achieve accurate water surface measurements using a point-gauge, therefore even a perfect numerical prediction would most probably show deviations when compared against physical measurements. Therefore, it can be said that the longitudinal water surface profiles were slightly over-predicted by the model.

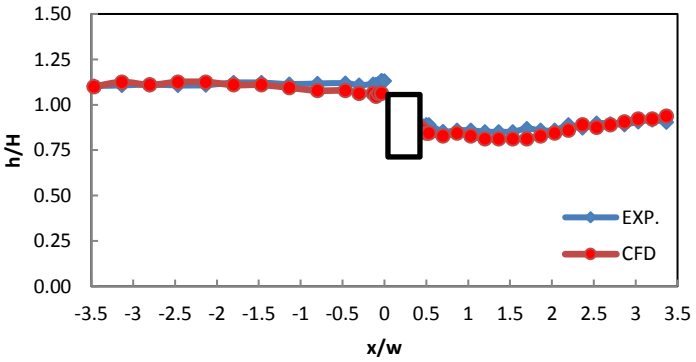

Fig. 3. Results of free surface flow profiles for CFD and experimental data for full orifice flow case (Q = 4.5 L/s).

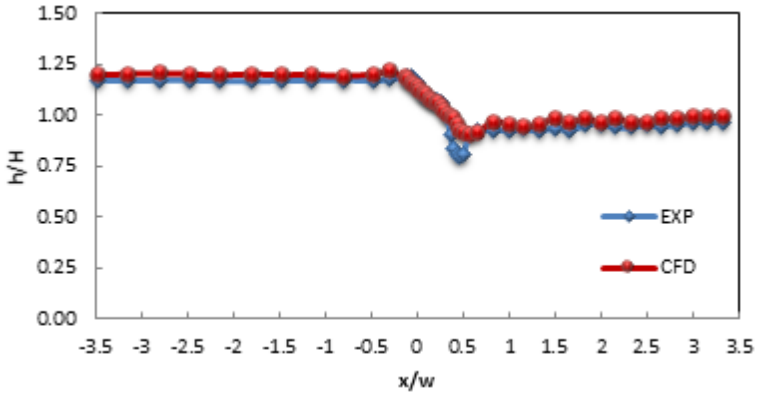

(a) Q = 7.0 L/s.

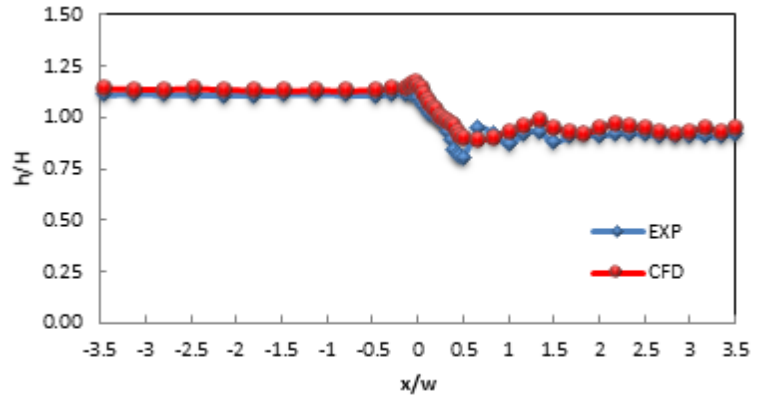

(b) Q =8.5 L/s.

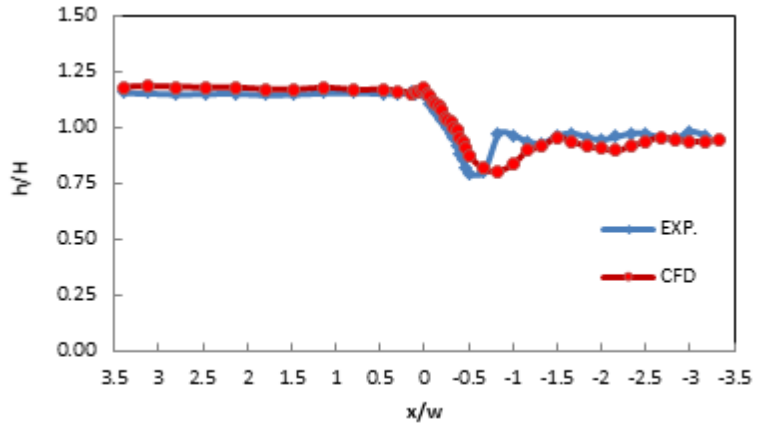

(c) Q = 12 L/s.

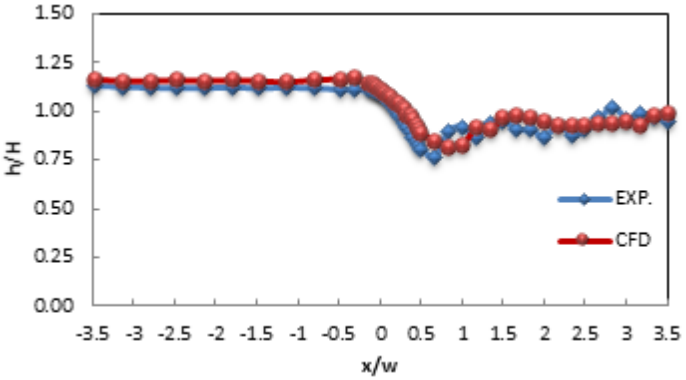

(d) Q = 15 L/s.

Fig. 4. Results of free surface flow profiles for CFD and experimental data for overtopping flow cases.

Figure 5 shows the distribution of longitudinal velocity resulted from the numerical model. Instantaneous velocity streamline plots in a longitudinal section at the middle of the bridge opening were considered for the orifice flow case study (see Fig. 5). Higher velocities were monitored at the bed of the full- orifice flow. With the overtopping case studies (see Figs. 6(a) to (d)), higher velocities with large eddies are highly fluctuating in nature after convergence of the velocity field reached a steady state. Very low mean velocity was observed in the flow separations upstream and downstream of the constriction. Flow velocity entering the constricted area increased rapidly. In the downstream part, high velocity remained in the main channel section due to the shear effect of flow separation extending to the outlet. Expectedly, it was observed that from the velocity distributions presented in Fig. 6 the temporarily higher velocities appear within the CFD model. This is because the model does indeed replicate the fluctuating nature of larger eddies. Eddies are highly distinguished in front of the bridge, over the deck and down-stream the bridge as shown in Figs. 6(a) to (d); the velocity dip (drop) in the main channel, resulting in a shift in the location of the maximum velocity below the water surface.

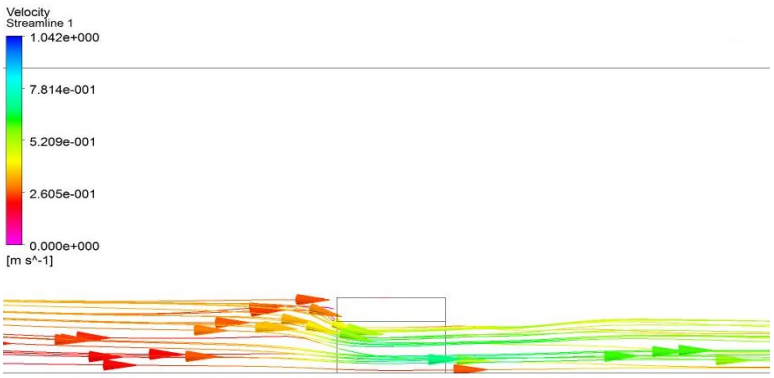

Fig. 5. Longitudinal velocity distribution resulted from the numerical model for orifice flow case (Q = 4.5 L/s).

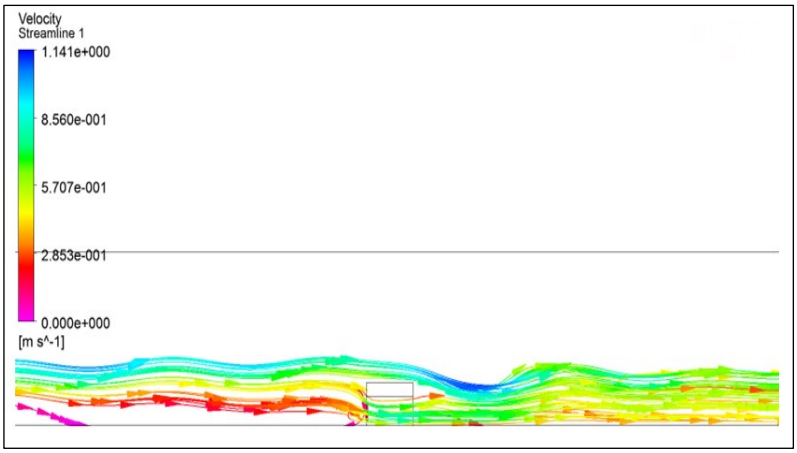

(a) Q = 7.0 L/s.

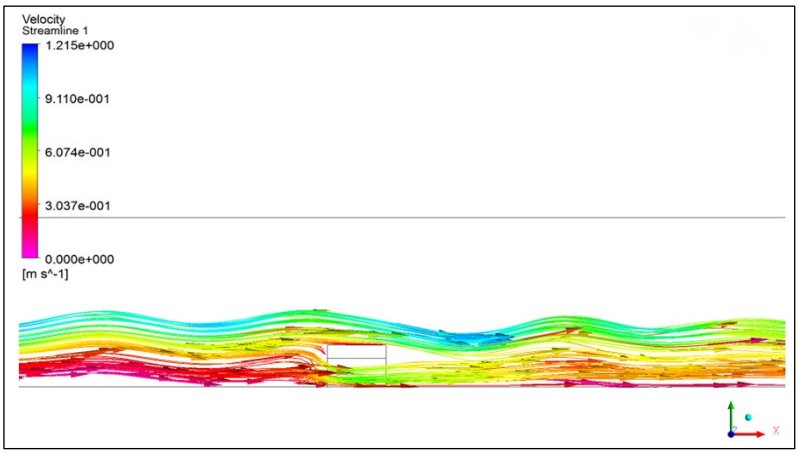

(b) Q = 8.5 L/s.

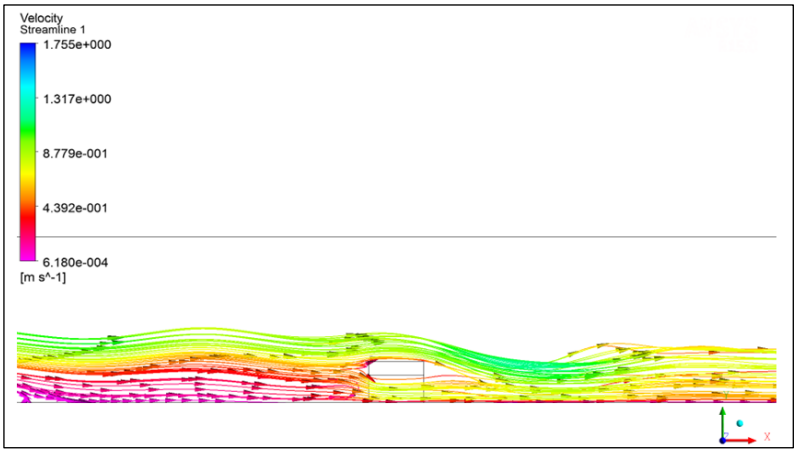

(c) Q = 12 L/s.

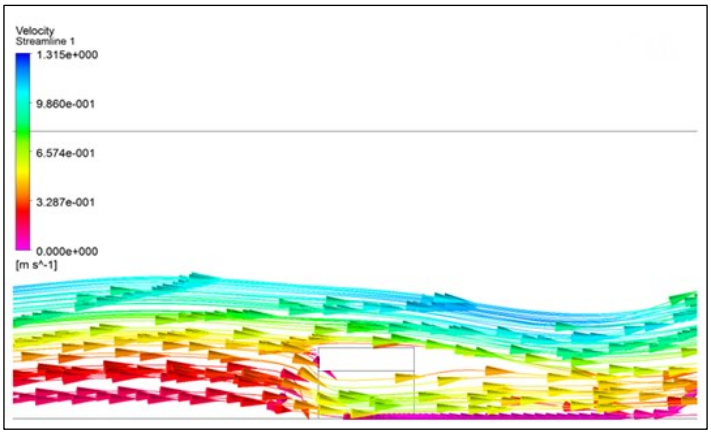

(d) Q = 15 L/s.

Fig. 6. Longitudinal velocity distribution resulted from numerical model for overtopping flow cases.

5. Conclusions

A three-dimensional CFD numerical model has been used to calculate the longitudinal velocity flow patterns and free surface profile to simulate that used in a laboratory flume experiment featuring open channel flow and a bridge obstruction. The model predictions were verified using experimental results obtained using a flume. Results are highlighted as water surface profiles and velocity field for two flow categories of full orifice flow and overtopping flow. One discharge of (4.5 L/s) was examined with the orifice flow and four discharges were tested with the overtopping cases. The comparisons between the predicted and measured water surface profiles data for both categories showed good agreement. However, with the overtopping case there was a significant shift between the numerical and the experimental cases at the downstream location at (12 L/s and 15 L/s) discharges due to the turbulence impact. Simulation was capable of capturing flow patterns and in this research it has been highlighted just in a velocity fields. Higher velocities were monitored at the bed of the full- orifice flow. While with the overtopping case, higher velocities with large eddies are highly fluctuating in nature after convergence of the velocity field reached a steady state. In addition, the captured eddies by the numerical model are highly distinguished in front of the bridge, over the deck and down-stream the bridge.

Acknowledgements

The authors would like to pay thank to the respectable Mustansiriyah University, Baghdad, Iraq (www.uomustansiriyah.edu.iq), and also thank to Cardiff University where the experiments works were carried out at the hydraulic laboratories of the University.

Nomenclatures

B	Bed width , m
C_μ	Constant

$C_{1\varepsilon}$	Constant
$C_{2\varepsilon}$	Constant
Fr	Froude number
H	Water depth (Fig. 1), cm
h	Water level along flume (Fig. 3), cm
k	Turbulent kinetic energy, m^2/s^2
p	Pressure N/m^2
Q	Discharge, L/s
Re	Reynolds number
t	Time, seconds
u	Velocity of flow
V_{uni}	Uniform velocity, m/s
w	Width of flume (Fig. 3), cm
x	Distance along flume (Fig. 3), cm

Greek Symbols

α□	Volume fraction of water (Fig. 2)
ε	Turbulent kinetic energy dissipation, m^2/s^3
μ_t	Turbulent eddy viscosity, $N/m^2.s$
ν	Kinematic viscosity, m^2/s
ρ	Density, kg/m^3
$\sigma\varepsilon$	Constant
σk	Constant
τ	Shear stress, N/m^2
τ_{ij}	Reynolds stress, N/m^2

Abbreviations

CFD	Computational Fluid Dynamics
RNG	Re-Normalization Group
VOF	Volume of Fluid

References

1. Koken, M.; and Constantinescu, G. (2009). An investigation of the dynamics of coherent structures in a turbulent channel flow with a vertical sidewall obstruction. *Physics of Fluids*, 21(8), 16 pages.
2. Oudenbroek, K.; Naderi, N.; Bricker, J.D.; Yang, Y.; van der Veen, C.; Uijttewaal, W.; Moriguchi, S.; and Jonkman, S.N. (2018). Hydrodynamic and debris-damming failure of bridge decks and piers in steady flow. *Geosciences*, 8(11), 26 pages.
3. Guo, J.; Admiraal, D.M.; and Zhang, T.C. (2010). Computational design tool for bridge hydrodynamic loading in inundated flows of Midwest Rivers. *Report # MATC-UNL: 227 Final Report 25-1121-0001-227*.
4. Malavasi, S.; and Guadagnini, A.; (2003). Hydrodynamic loading on river bridges. *Journal of Hydraulic Eng*ineering, 129(11), 854-861.
5. Kerenyi, K.; Sofu, T.; and Guo, J. (2009). *Hydrodynamic forces on inundated bridge decks.* Publication no. FHWA-HRT-09-028. Federal Highway Administration: McLean, Virginia, Washington D.C., United States of America.

6. Hong, S.H.; and Sturm, T.W. (2010). Physical modeling of abutment scour for overtopping submerged orifice and free surface flows. *Proceedings of the Fifth International Conference on Scour and Erosion*. San Francisco, California, United States of America, 590-.
7. Hong, S.H.; and Lee, S.O. (2018). Insight of bridge scour during extreme hydrologic events by laboratory model studies. *KSCE Journal of Civil Engineering*, 22(8), 2871-2879.
8. Sturm, T.W.; Ettema, R.; and Melville, B.W. (2011). Evaluation of bridge-scour research: Abutment and contraction scour processes and prediction. Washington, D.C.: Transportation Research Board.
9. Martin-Vide, J.P.; and Prio, J.M. (2005). Backwater of arch bridges under free and submerged conditions. *Journal of Hydraulic Research*, 43(5), 515-521.
10. Picek, T.; Havlik, A.; Mattas, D.; and Mares, K. (2007). Hydraulic calculation of bridges at high water stages. *Journal of Hydraulic Research*, 45(3), 400-406.
11. Lee, D.; Nakagawa, H.; Kawaike, K.; Baba, Y.; and Zhang, H. (2010). Inundation flow considering overflow due to water level rise by river structures. *Annuals Disaster Prevention Research Institute*, 53(B), 607-616.
12. Li, G.; Lang, L.; and Ning, J. (2013). 3D Numerical simulation of flow and local scour around a spur dike. *Proceedings of IAHR World Congress*. Chengdu, China, 9 pages.
13. Kara, S.; Mulahasan, S.; Stoesser, T.; and Sturm, T.W. (2014). Water surface response to flow through bridge opening. *Proceedings of the 7th International Conference on Fluvial Hydraulics (River Flow). Lausanne, Switzerland,* 1-8.
14. Kara, S.; Stoesser, T.; Strum, T.W.; and Mulahasan, S. (2015). Flow dynamics through a submerged bridge opening with overtoping. *Journal of Hydraulic Research,* 53(2), 186-195.
15. Yazdi, J.; Sarkardeh, H.; Azamathulla, H.M.; and Ghani, A.A. (2010). 3D simulation of flow around a single spur dike with the free-surface flow. *International Journal of River Basin Management*, 8(1), 55-62.
16. Ketong, L.; Aiping, T.; Yuejun, L.; and Hao, Z. (2015). Flutter analysis for bridge decks using Lattice Boltzmann Method. *Engineering Review*, 35(3), 223-237.
17. Fleit, G. (2016). *Validation of a 3D morphodynamic model for complex* flows. Master Thesis. Department of Hydraulic and Water Resources Engineering, Budapest University of Technology and Economics, Budapest, Hungary.
18. Haun, S.; Olsen, N.R.B.; and Feurich, R. (2011). Numerical modelling of flow over a trapezoidal broad-crested weir. *Engineering Applications of Computational Fluid Mechanics*, 5(3), 397-405.
19. Hong, S.H.; and Abid, I. (2016). Physical model study of bridge contraction scour. *KSCE Journal of Civil Engineering*, 20(6), 1-8.
20. Yoon, K.S.; Lee, S.O.; and Hong, S.H. (2019). Time-averaged turbulent velocity flow field through various bridge contractions during large flooding. *Water*, 11(1), 13 pages.

21. Mulahasan, S. (2016). *Hydrodynamics of large-scale roughness in open channels.* Ph.D. Thesis. School of Engineering, Cardiff University, Cardiff, United Kingdom.
22. Yakhot, V.; and Orszag, S.A. (1986). Renormalization group analysis of turbulence. I. Basic theory. *Journal of Scientific Computing*, 1, 3-51.
23. Launder, B.E.; and Spalding, D.B. (1974). The numerical computation of turbulent flows. *Computer Methods in Applied Mechanics and Engineering*, 3(2), 269-289.
24. Hirt, C.W.; and Nichols, B.D. (1981). Volume of fluid (VOF) method for the dynamics of free bound- arise. *Journal of Computational Physics*, 39, 201-225.